Temperature and radiation measurements of an atmospheric pressure CO2 plasma

Corentin H C Grimaldi, Sean Mcguire, Augustin Tibère-Inglesse, Christophe O Laux

Temperature and radiation measurements of an atmospheric pressure CO_2 plasma

Corentin H. C. Grimaldi[1], Sean McGuire[2], Augustin Tibère-Inglesse[3] & Christophe O. Laux[4]

Laboratoire EM2C, CNRS UPR288, CentraleSupélec, Université Paris-Saclay, 3 rue Joliot Curie, 91190 Gif-sur-Yvette, France

An atmospheric pressure CO_2/Ar plasma is produced using an ICP torch. This plasma is passed at high velocity through a water-cooled test-section that forces rapid cooling and recombination. At the water-cooled test-section inlet, the plasma is close to Local Thermodynamic Equilibrium at about 6750 K. The subsequent thermochemical evolution of the plasma at it traverses the water-cooled tube is studied using Optical Emission Spectroscopy from the UV to NIR. The measured spectra, calibrated in absolute intensity, are compared with calculations done using the SPECAIR line-by-line radiation code. At the exit of the 15-cm water-cooled tube, the centerline temperature is found to have dropped to 6100 K. Indications of thermochemical non-equilibrium are found in the emission spectrum at the exit of the tube. The measurements presented here are meant to provide a test case for comparison with theoretical predictions made by kinetic models and/or CFD predictions.

I. Introduction

The entry of a space vehicle into the atmosphere of a planet or a satellite occurs at hypersonic velocities. The resulting shock wave that forms in front of the vehicle can heat the surrounding gas to temperatures of 10,000K, leading to intense gas heating and the formation of a plasma in the post-shock region. The study of the convective and radiative heat fluxes resulting from this plasma is critical for the design of the thermal protective system (TPS) and therefore the mission [1]. The atmosphere of Mars (by mole fraction: CO_2: 96.0%, Ar: 1.93%, N_2: 1.89%) [2] and the atmosphere of Venus (by mole fraction: CO_2: 96.5%, N_2: 3.5%) [3] are composed principally of CO_2 with lesser quantities of N_2 and Ar. The orbital mechanics associated with an Earth to Mars transit dictate relatively low entry velocities into the Martian atmosphere (< 8.5 km/s) [4]. This is to be compared with Earth entry velocities that can be as high as 15 km/s for a Mars return scenario [5]. The relatively low entry velocity and the small entry vehicle sizes have previously led engineers to neglect the radiative heat flux. However, for larger entry vehicle sizes or for higher velocities such as into the atmosphere of Venus (< 11 km/s), the radiative heat flux to the capsule surface becomes more important, both in the forebody and afterbody regions [6]–[8].

Beginning in the late 90s, work began to determine the importance of the radiative heat flux for both forebody and afterbody heating predictions. For example, as part of the Mars PREMIER program (1998-2003) supported by CNES (Centre National d'Études Spatiales), a Martian entry vehicle geometry test case known as TC3 was simulated [9]. The analysis of the results showed that the radiative heat fluxes in the afterbody region generally exceeded the convective heat fluxes [9]. Afterwards, other simulations were also conducted to try and quantify the impact of radiative heating for Mars entry. In 2011, da Silva [10] carried out an analysis on the entry phase of the ESA (European Space Agency) ExoMars mission with special attention to both forebody and afterbody radiative heat fluxes. He found out that the radiative and convective fluxes were roughly equivalent in the afterbody region. More recent simulations of the radiative heat fluxes on vehicles entering the Mars atmosphere were conducted in 2013 by Mazaheri et al. [11] and in 2015 by Brandis et al. [7]. Both studies showed that radiative heating in the afterbody often exceeds convective heating and therefore must be considered for TPS design for future Martian missions. In 2012, NASA landed the Mars Science Laboratory (MSL) including the Curiosity Rover. The TPS of

[1] Ph.D. Student, Laboratoire EM2C, CNRS UPR288, CentraleSupélec, Université Paris Saclay

[2] Assistant Professor, Laboratoire EM2C, CNRS UPR288, CentraleSupélec, Université Paris Saclay, AIAA Member

[3] Postdoctorate, Laboratoire EM2C, CNRS UPR288, CentraleSupélec, Université Paris Saclay

[4] Professor, Laboratoire EM2C, CNRS UPR288, CentraleSupélec, Université Paris Saclay, AIAA Associate Fellow

the capsule contained the MSL Entry Descent Landing System (MEDLI) suite, which included the MEDLI integrated sensor plugs (MISPs) measuring the in-depth temperature using thermocouples located on the forebody heat shield. Cruden et al. [12] found that the heat load was 33% lower than the postflight prediction with the convective heating alone, the difference being attributed to radiation from the shock heated gas. In 2016, for the first time, the radiative heat flux during Martian entry was measured by the Combined Aerothermal and Radiometer Sensor (COMARS+) on the back cover of the ExoMars Schiaparelli capsule. The radiative contribution to the total heat flux on the back shell was up to 61% after the blackout phase [13]. These measurements confirm the previous findings that radiative heating can be a significant part of the total heat flux on the back cover.

The examples from the preceding paragraph highlight the importance of a better understanding and prediction of the radiative heat flux, particularly in the afterbody region. The radiative heat flux to the afterbody suffers from large uncertainties from 50% to 260% for Mars entry scenarios [14]. The rapid hydrodynamic expansion of the plasma into the afterbody results in rapid cooling, chemical recombination and a departure from equilibrium [8]. This chemical non-equilibrium and the associated radiation are still not accurately modeled, and our goal is to provide experimental data to help reduce this uncertainty. To accomplish this, it is necessary to understand the recombination dynamics of CO_2 plasmas – specifically, the recombination kinetics [15]. The work here represents part of an effort to define a recombining CO_2 plasma test case and provide initial measurements in the UV-visible region looking at the recombination dynamics.

II.Experimental Setup

The plasma torch facility at laboratoire EM2C produces atmospheric pressure plasmas at temperatures ranging between 6000 and 9000K. The plasma torch employed is a TAFA Model 66 Inductively Coupled Plasma (ICP) torch powered by a 120kVA radio frequency LEPEL Model T-50-3 power supply that operates at 4MHz. Although the facility can deliver 50 kW into the plasma flow, during the current experiments, a low-power condition was studied, at a plate power of 40 kW. More details of the plasma torch facility may be found in several references: [16]–[18]. The CO_2 plasma studied here exits the torch through a 1-cm diameter nozzle at a speed between 500 m/s and 700 m/s and is composed of 0.395 g/s ±2% of carbon dioxide premixed with 3.10 g/s ±2% of argon to provide stable and sustainable operating conditions. Consequently, the mass fractions of the mixture are respectively 11% for CO_2 and 89% for Ar. For this injection mixture, approximately 60% of the mixture was injected via the radial injectors, 34% via the swirl injectors and the remaining 7% was injected via the axial injectors. Water-cooled test-sections of various lengths are placed on the 1-cm diameter exit of the torch in order to provoke rapid cooling and therefore force plasma recombination in a well-controlled environment. Figure 1 shows a schematic of the experimental set-up for Optical Emission Spectroscopy (OES) and temperature measurements.

.

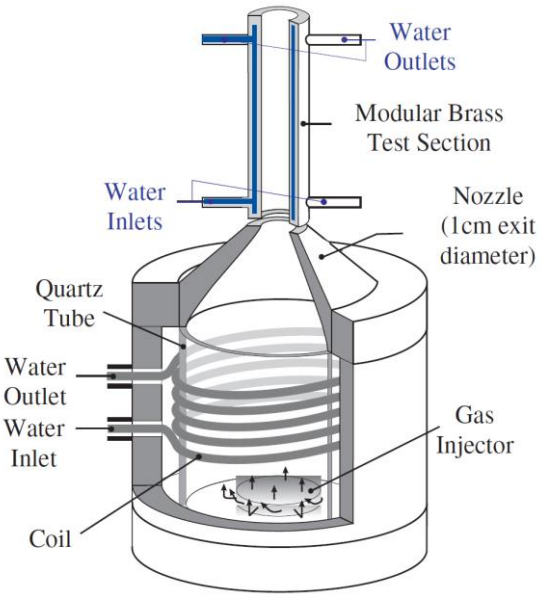

Figure 1. Schematic of ICP torch head with non-equilibrium test-section for CO_2 recombination experiments.

The OES measurements in the UV and in the visible region were performed directly at the exit of the torch or the test-sections with a 0.75 m focal length spectrometer (Princeton Instruments Acton SpectraPro 2750i) fitted with a 1024x256 pixels CCD camera (Princeton Instruments PI-MAX II). Second- and higher order light was rejected

with 300 and 550 nm long pass filters, depending on the targeted wavelength region. Spectra from 240 to 855nm were made using the experimental setup presented in Figure 2 at the exit of the ICP torch and at the exit of the 5 and 15 cm test-sections. The spectral resolution of the system (Full Width at Half Maximum (FWHM of the slit function) was 0.27 nm.

Absolute calibrations of the spectral intensities were made using radiance standards (traceable to NIST standards), including a 1-kW argon mini-arc in the UV region [19] and a calibrated tungsten lamp (Optronics Laboratory OL 550) equipped with a sapphire window for the visible and near IR regions. These calibration standards overlap in the 350-400 nm region. We are currently seeing a discrepancy between the two calibrations in this overlap region. The calibration via the argon mini-arc is very sensitive to alignment since the arc discharge emission is calibrated over a limited solid angle at the exit of the arc. The tungsten lamp is less sensitive to small misalignments. We therefore attribute the discrepancy to a misalignment of the argon discharge and apply a correction factor to this calibration so that it agrees with the calibration via the tungsten lamp in the overlap region of 350 – 400 nm. This correction only impacts the spectrum below 400 nm and much of the results are above this wavelength.

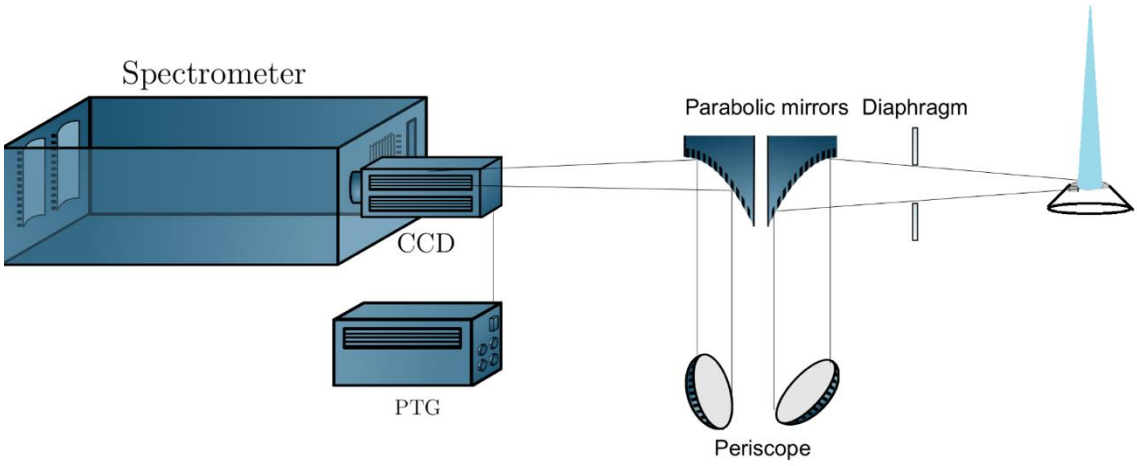

Figure 2 Schematic of the experimental setup used for UV, visible and near IR Optical Emission Spectroscopy (OES)**.**

III.Results

As explained in detail in Ref. [20], for a plasma in Local Thermodynamic Equilibrium (LTE), the integrated intensity I of a spectral line between an excited electronic level u and a lower level l is related to the LTE temperature T_{LTE} and the pressure P by:

$$I = \frac{A_{ul}}{4\pi}(\varepsilon_u - \varepsilon_l)X_s(T_{LTE})\frac{P}{kT_{LTE}}\frac{g_u}{Q_{el}(T_{LTE})}\exp\left(-\frac{\varepsilon_u}{kT_{LTE}}\right) \qquad \textbf{Equation 1}$$

where A_{ul} is the Einstein coefficient, g_u is the degeneracy of the upper level and ε_u and ε_l the upper and lower energies. Q_{el} and X_s are respectively the electronic partition function and the mole fraction of the atom s. If the plasma is in LTE, the LTE temperature characterizes the electronic distribution and can be inferred from measurements of integrated intensity of any spectral line using Equation 1. If the electronic levels do not follow a Boltzmann distribution with respect to the ground state, each atomic line yields a different temperature. In this case, the different temperatures inferred have no physical meaning and only indicate a departure from equilibrium.

Special attention was given to the uncertainty analysis, the total relative error on the LTE temperature is given by:

$$\left|\frac{\Delta T_{LTE}}{T_{LTE}}\right| = \frac{kT_{LTE}}{\varepsilon_u + kT_{LTE}}\left(\left|\frac{\Delta I}{I}\right| + \left|\frac{\Delta A_{ul}}{A_{ul}}\right| + \left|\frac{\Delta X_s}{X_s}\right| + \left|\frac{\Delta P}{P}\right|\right) \qquad \textbf{Equation 2}$$

In Equation 2, the two major sources of uncertainty are the Signal to Noise Ratio (SNR) of the experimental measurements and the accuracy of the Einstein coefficients. Depending on the spectral line, these Einstein coefficient accuracies vary from 3% to 10%. The uncertainty on the mole fraction of the atom is impacted by the accuracy of the flowmeters and remains less than 2% over the possible temperature range. The uncertainty on the pressure is negligible. The combined uncertainty on the temperature measurements remains less than 2% at the center of the plasma.

The radial temperature profiles presented in the following sections were obtained by measuring the absolute intensity of atomic lines of Carbon (833.5 nm), Oxygen (777 nm and 844 nm) and Argon (763.5 nm, 811.5 nm and 842.4 nm). These intensities are Abel-inverted to obtain their radially resolved emission. The NASA CEA code [21] was used to determine the equilibrium mole fractions of the gas mixture as a function of temperature. Then using the constants associated with the spectral line and the operating conditions, the intensity of the measured lines is calculated as a function of temperature and compared with the measurements in order to have the LTE temperature. The complete procedure is detailed in [16].

The absolute intensity emission spectra obtained by OES measurements between 240 and 855 nm were Abel-inverted to show in the following sections the centerline values of the experimental OES measurements, compared to simulations of CO_2/Ar plasma emission at LTE (using the center value of the temperature measurements) using the SPECAIR code [16], [22]. The current version of SPECAIR models 37 molecular transitions of NO, N_2, N_2^+, O_2, CN, OH, NH, C_2 and CO, as well as atomic lines of N, O, C and Ar. The plasma conditions are those corresponding to the temperature profiles measured using atomic spectral lines. In the sections that follow, both the temperature measurements and OES spectra will be presented for several water-cooled test-section lengths: beginning directly at the exit of the torch with no water-cooled tube and ending with a test-section length of 15 cm.

A. Temperature and OES measurements – exit of the torch

Figure 3 shows all temperature measurements from several lines of carbon, oxygen and argon measured at the exit of the torch, which corresponds to the entrance of the water-cooled tube. On centerline, the temperatures are all equal to within their uncertainty and yield a temperature of 6750K±60K. Beginning at approximately 0.25 cm radial distance (half of the radius of the plasma), the temperature from the carbon 833.5 nm line begins to differ from the other temperature estimates. This has been observed to be reproducible across several experiments. For the OES measurements that follow, a maximum and minimum intensity will be calculated based upon the maximum and minimum possible temperature profiles which bound the shaded grey region in Figure 3. The black and shaded red spectra are respectively the experimental OES measurement and the SPECAIR predictions.

Figure 4 - 6 show the comparison between the OES measurements and the SPECAIR predictions. A small continuum of 0.02mW/cm^3/nm/sr was added to the SPECAIR calculation. Even if the gas mixture injected in the plasma torch was comprised only of argon and carbon dioxide, the experimental spectrum reveals the presence of CN. This is due to mixing of ambient nitrogen into the plasma at the edge of the jet. A small fraction of air (about 0.5%) was added to the simulated mixture to match the contribution from the CN Violet vibrational bands present between 350 and 425 nm. Figure 6 show that the intensities of all observed atomic lines between 655 and 855 nm lie within the uncertainty bounds. However, Figure 5 shows that the C_2 Swan vibrational bands between 425 and 625 nm do not fit perfectly with the prediction. Decreasing the translational/rotational temperature by 200 K results in a much better fit to these features; as shown Figure 7.

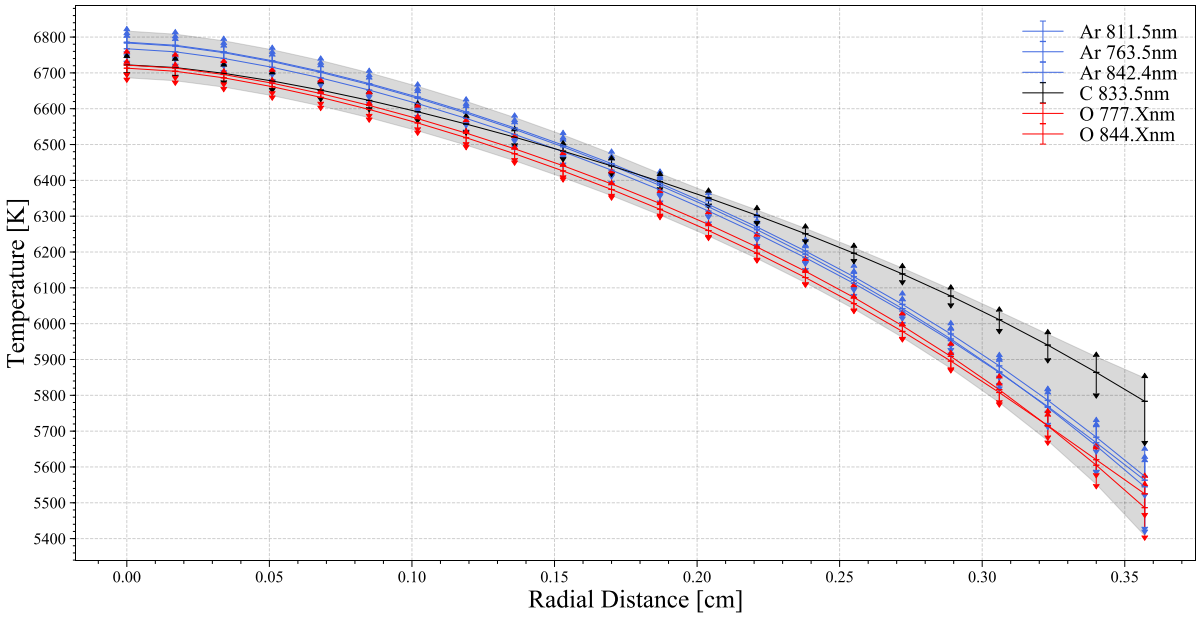

Figure 3 Temperature measurements using argon, carbon and oxygen lines at the exit of the torch.

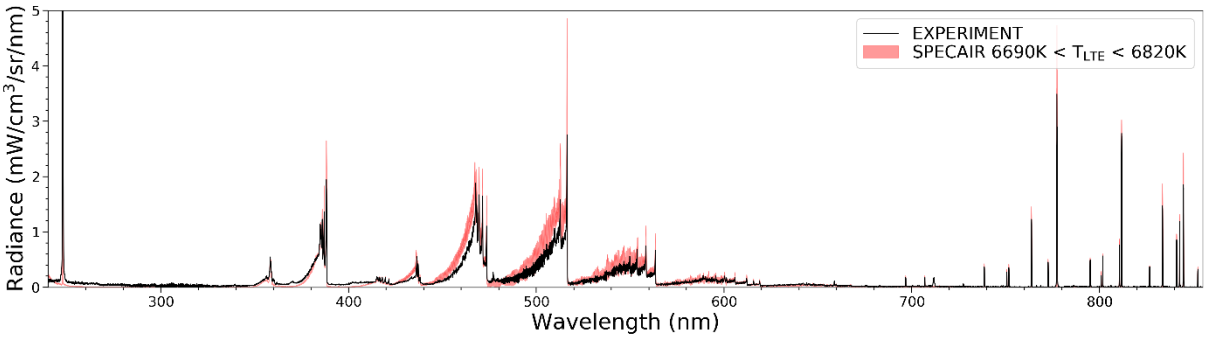

Figure 4 Comparison between experimental spectrum and SPECAIR prediction at the exit of the torch between 240 and 855 nm with 6690 < T_{LTE} < 6820 K.

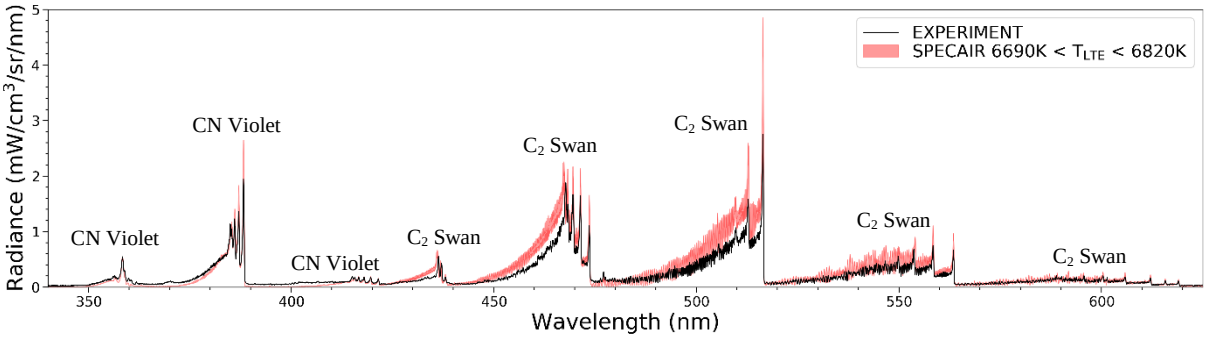

Figure 5 Comparison between experimental spectrum and SPECAIR prediction at the exit of the torch over the CN Violet and C_2 Swan vibrational bands 6690 < T_{LTE} < 6820 K.

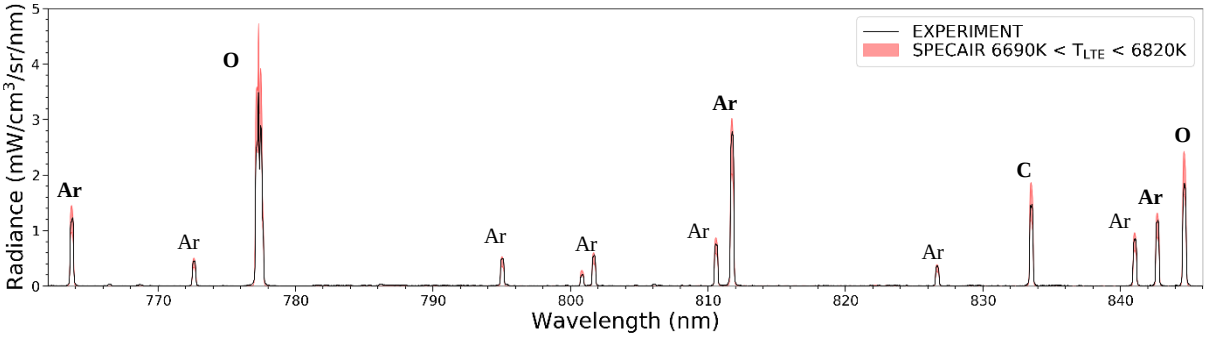

Figure 6 Comparison between experimental spectrum and SPECAIR prediction at the exit of the torch of the atomic lines of argon, carbon and oxygen 6690 < T_{LTE} < 6820 K.

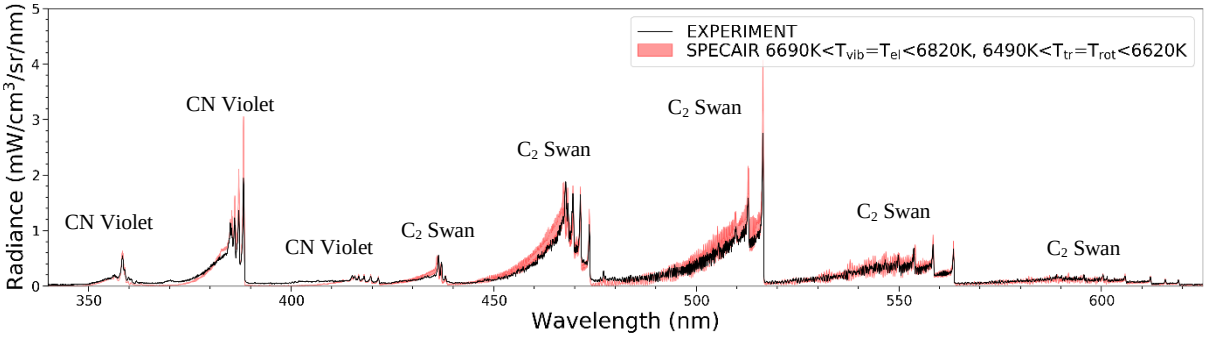

Figure 7 Comparison between experimental spectrum and SPECAIR prediction at the exit of the torch over the CN Violet and C_2 Swan vibrational bands with 6690 < T_{vib} = T_{el} < 6820 K and a slightly reduced temperature translational/rotational temperature of 6490 < T_{tr}=T_{rot} < 6620 K.

B. Temperature and OES measurements – 5-cm test-section

Temperature measurements at the exit of the 5-cm water-cooled tube, for the same inlet conditions, are shown in Figure 8. All argon, carbon and oxygen atomic lines are once again in good agreement at the center of the plasma and provide a centerline temperature of 6420±80 K. As compared with the temperature measurements directly at the exit of the torch, the plasma has cooled by approximately 330 K. The same discrepancy between the 833.5 nm carbon temperature profile and the other atomic lines is also observed here. Figure 9 and 10 show the spectrum obtained by OES measurements. All observed features appear to fall within the uncertainty on the intensity resulting from the temperature uncertainty.

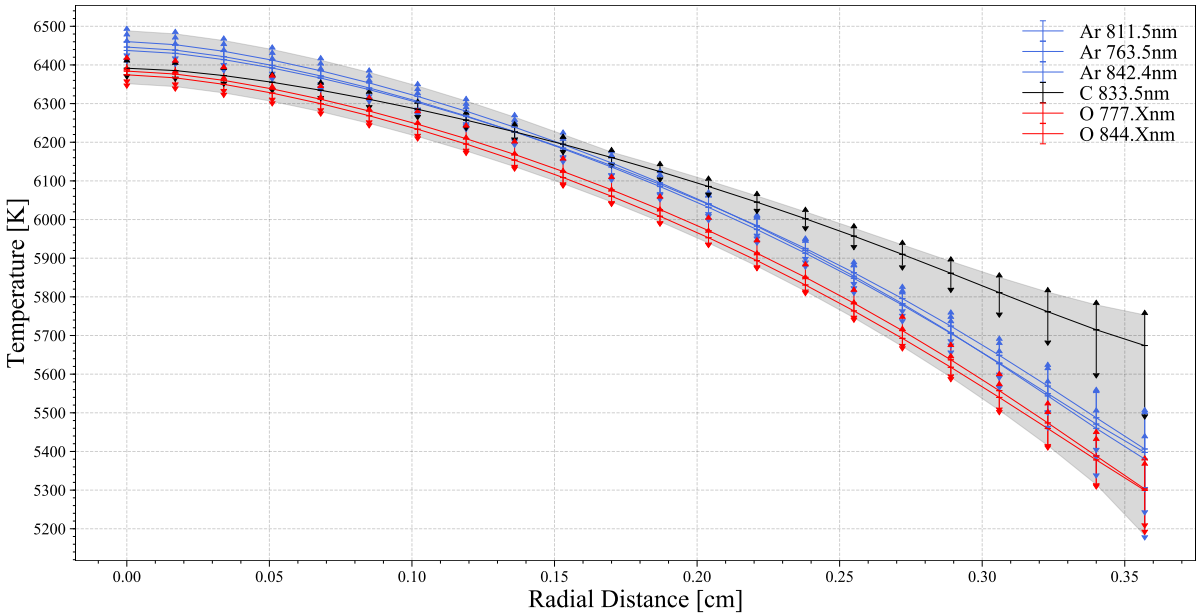

Figure 8 Temperature measurements using argon, carbon and oxygen lines at the exit of the 5cm test-section.

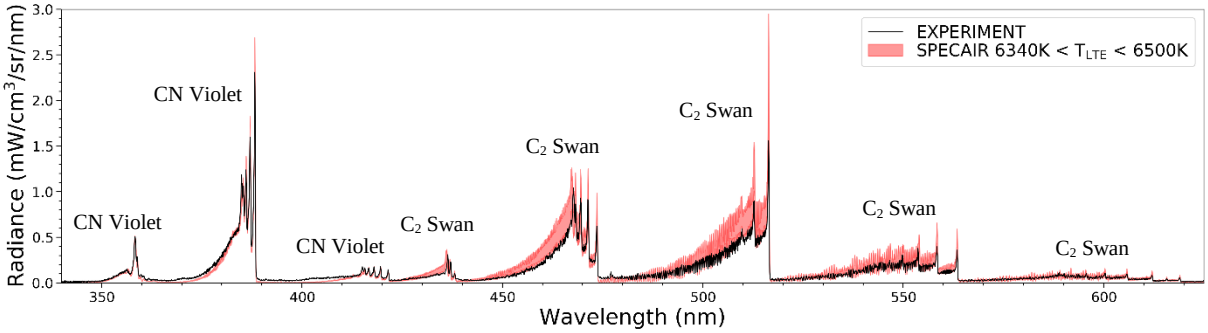

Figure 9 Comparison between experimental spectrum and SPECAIR prediction at the exit of the 5cm test-section over the CN Violet and C2 Swan vibrational bands 6340K<T_{LTE}<6500K.

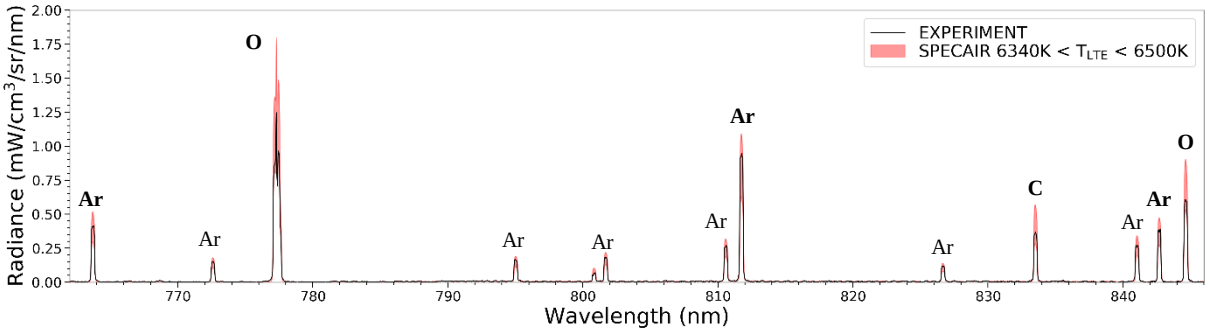

Figure 10 Comparison between experimental spectrum and SPECAIR prediction at the exit of the 5cm test-section of the atomic lines of argon, carbon and oxygen 6340K<T_{LTE}<6500K.

C. Temperature and OES measurements – 15cm test-section

At the exit of the 15cm test-section, the temperature measurements obtained from several atomic transitions show significant discrepancies, as shown in Figure 11, thus indicating a departure from equilibrium. The average temperature measured at the center of the plasma is 6090±80 K. The temperature is approximately 650 K cooler than at the entrance to the water-cooled tube. Figure 12 and 13 show the comparison between the SPECAIR predicted spectrum and the experimental one obtained by OES. C_2 Swan emission is clearly outside the boundaries of the SPECAIR calculation assuming LTE. These disagreements indicate that the plasma is out of equilibrium at the exit of the 15cm test-section.

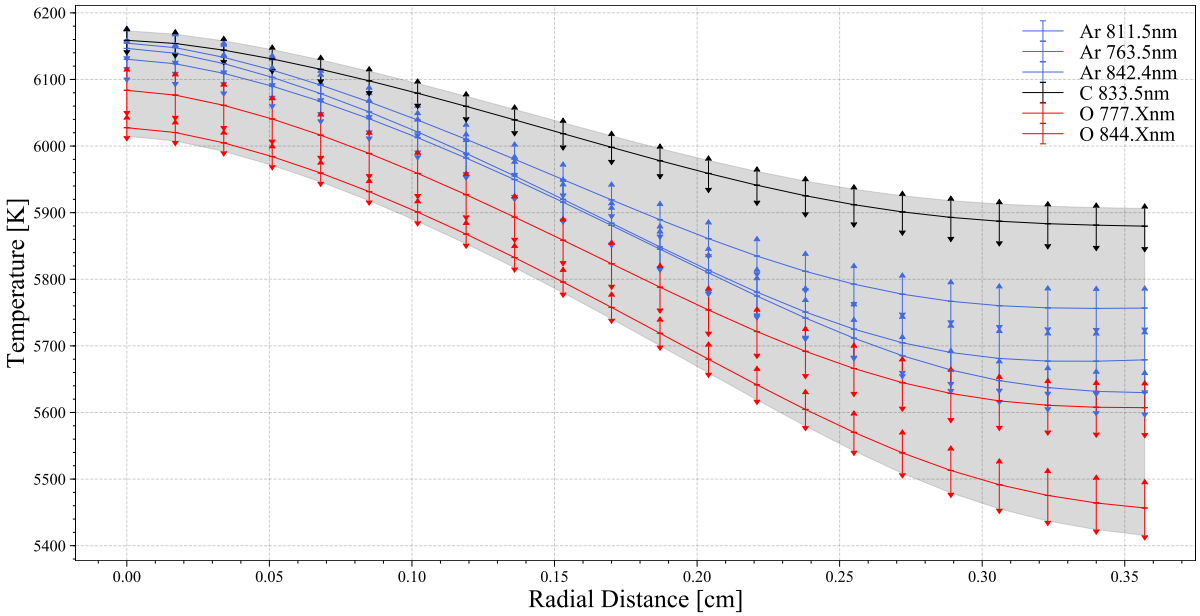

Figure 11 Temperature measurements using argon, carbon and oxygen lines at the exit of the 15cm test-section.

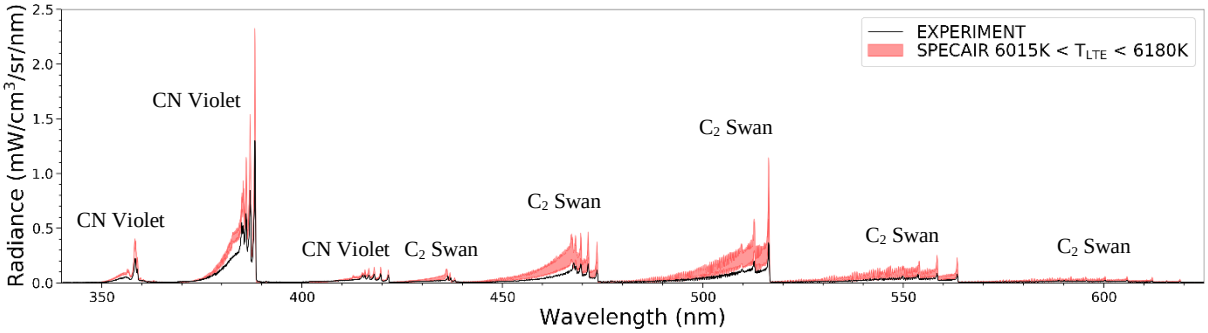

Figure 12 Comparison between experimental spectrum and SPECAIR prediction at the exit of the 15cm test-section over the CN Violet and C2 Swan vibrational bands 6015<T_{LTE}<6180K.

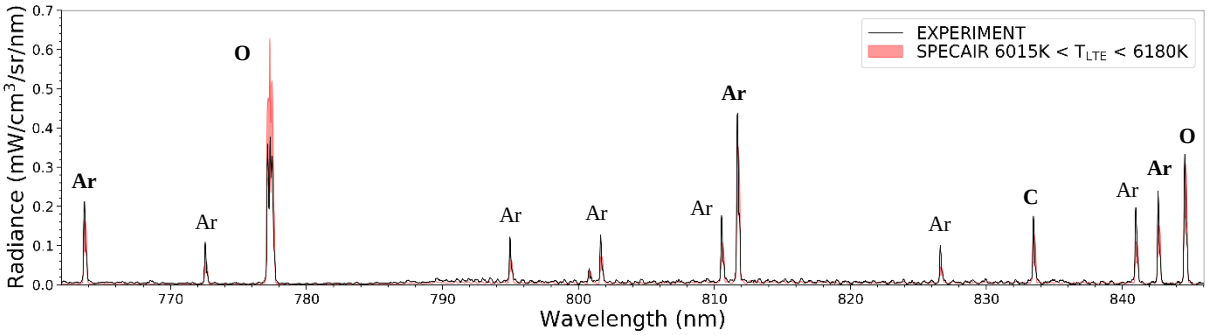

Figure 13 Comparison between experimental spectrum and SPECAIR prediction at the exit of the 15cm test-section of the atomic lines of argon, carbon and oxygen 6015K<T_{LTE}<6180K.

IV.Conclusion

The work presented here will be continued in the UV-visible region for different test-section lengths. Temperature and OES measurements will be made at intermediate tube lengths between 5 and 15 cm in order to quantify the departure from equilibrium. Water-cooled test-sections above 15 cm will also be investigated (current maximum test-section length is 80 cm) to observe what happens as the plasma is continually cooled and, in particular, to see if the plasma remains close to LTE conditions or departs from equilibrium as is the case for previous N_2/Ar mixtures studied using this configuration [17], [23]. Figure 14 shows that, below 4000 K, the O_2 and CO_2 mole fractions become important (>1%). Further work will be done to expand the measurement range into the infrared regions up to 5μ m to measure the CO_2 and CO infrared bands. We intend to therefore pursue optical emission spectroscopy measurements from 200 nm to 5μm – spanning the UV, visible and infrared spectral regions – in order to provide a comprehensive dataset for model validation purposes. To complete this dataset, power balance measurements will also be performed. For these, the water temperatures at the inlet and outlet of the water-cooled tube are measured and used to calculate the enthalpy removed from the plasma. This drop-in enthalpy can then be compared with estimates based upon the thermochemical state of the plasma at the inlet and exit of the water-cooled tube as a consistency check.

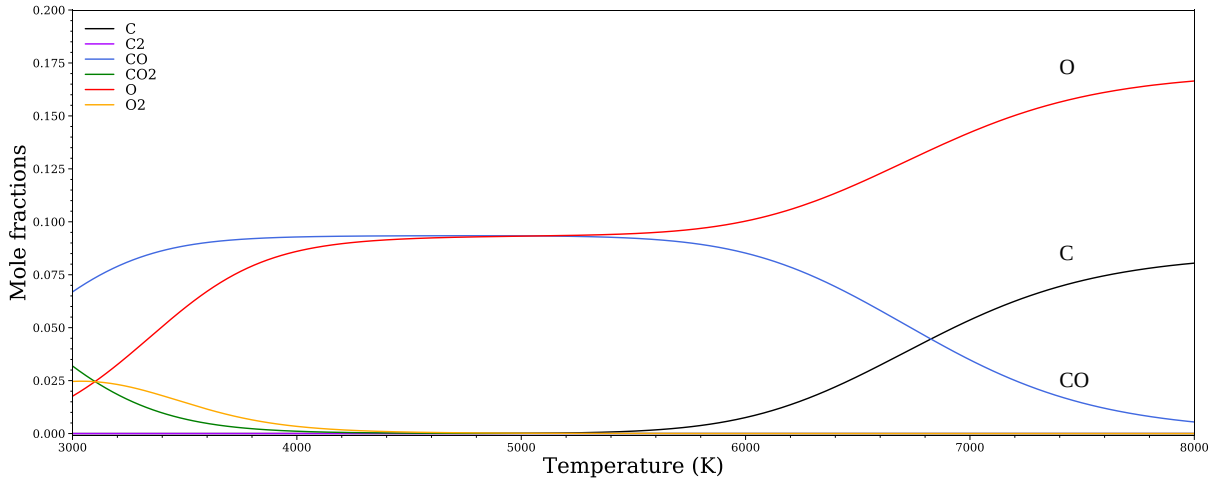

Figure 14 Equilibrium mole fractions of species in an LTE CO_2/Ar plasma between 3000 and 8000 K at 1 atm.

V. References

[1] I. Cozmuta, M. J. Wright, B. Laub, and W. H. Willcockson, "Defining ablative thermal protection system margins for planetary entry vehicles," *42nd AIAA Thermophys. Conf.*, no. June, pp. 1–27, 2011.

[2] Dr. David R. Williams, "Mars Fact Sheet," 2018. [Online]. Available: https://nssdc.gsfc.nasa.gov/planetary/factsheet/marsfact.html. [Accessed: 01-Oct-2019].

[3] Dr. David R. Williams, "Venus Fact Sheet," 2018. [Online]. Available: https://nssdc.gsfc.nasa.gov/planetary/factsheet/venusfact.html. [Accessed: 01-Oct-2019].

[4] B. A. Cruden, D. Prabhu, and R. Martinez, "Absolute Radiation Measurement in Venus and Mars Entry Conditions," *J. Spacecr. Rockets*, vol. 49, no. 6, pp. 1069–1079, 2012.

[5] C. O. Johnston, A. Mazaheri, P. Gnoffo, B. Kleb, and D. Bose, "Radiative heating uncertainty for hyperbolic earth entry, part 1: Flight simulation modeling and uncertainty," *J. Spacecr. Rockets*, vol. 50, no. 1, pp. 19–38, 2013.

[6] J. H. Grinstead, M. J. Wright, D. W. Bogdanoff, and G. A. Allen, "Shock Radiation Measurements for Mars Aerocapture Radiative Heating Analysis," *J. Thermophys. Heat Transf.*, vol. 23, no. 2, pp. 249–255, 2009.

[7] A. M. Brandis, D. A. Saunders, C. O. Johnston, B. A. Crudeny, and T. R. White, "Radiative heating on the after-body of martian entry vehicles," *45th AIAA Thermophys. Conf.*, vol. 94035, pp. 1–19, 2015.

[8] C. O. Johnston and M. Panesi, "Advancements in afterbody radiative heating simulations for earth entry," *46th AIAA Thermophys. Conf.*, no. June, pp. 1–19, 2016.

[9] R. Bonneville, F. Rocard, and J. L. Counil, "French involvement in Mars exploration," *Acta Astronaut.*, vol. 51, no. 1–9, pp. 329–335, 2002.

[10] M. L. Silva and J. Beck, "AIAA 2011 – XXXX Contribution of CO 2 IR Radiation to Martian Entries

Radiative Wall Fluxes 49th AIAA Aerospace Sciences Meeting Contribution of CO 2 IR Radiation to Martian," *New Horizons*, no. January, 2011.
[11] A. Mazaheri, C. O. Johnston, and S. Sefidbakht, "Three-dimensional radiation ray-tracing for shock-layer radiative heating simulations," *J. Spacecr. Rockets*, vol. 50, no. 3, pp. 485–493, 2013.
[12] B. A. Cruden, A. M. Brandis, T. R. White, M. Mahzari, and D. Bose, "Radiative Heating During Mars Science Laboratory Entry: Simulation, Ground Test, and Flight," *J. Thermophys. Heat Transf.*, vol. 30, no. 3, pp. 642–650, 2016.
[13] A. Gülhan, T. Thiele, F. Siebe, R. Kronen, and T. Schleutker, "Aerothermal measurements from the Exomars Schiaparelli capsule entry," *J. Spacecr. Rockets*, vol. 56, no. 1, pp. 68–81, 2019.
[14] C. O. Johnston, A. M. Brandis, and K. Sutton, "Shock layer radiation modeling and uncertainty for mars entry," *43rd AIAA Thermophys. Conf. 2012*, no. June, pp. 1–43, 2012.
[15] J. Annaloro, A. Bultel, and P. Omaly, "Detailed kinetic of CO2 dissociation and C ionization: Application to atmospheric Martian entries," *J. Phys. Conf. Ser.*, vol. 511, no. 1, 2014.
[16] C. O. Laux, T. G. Spence, C. H. Kruger, and R. N. Zare, "Optical diagnostics of atmospheric pressure air plasmas--- Stanford University.pdf," vol. 12, pp. 125–138, 2003.
[17] C. O. Laux, L. Pierrot, and R. J. Gessman, "State-to-state modeling of a recombining nitrogen plasma experiment," *Chem. Phys.*, vol. 398, no. 1, pp. 46–55, 2012.
[18] M. E. MacDonald, C. M. Jacobs, C. O. Laux, F. Zander, and R. G. Morgan, "Measurements of air plasma/ablator interactions in an inductively coupled plasma torch," *J. Thermophys. Heat Transf.*, vol. 29, no. 1, pp. 12–23, 2015.
[19] J. Z. Klose, J. M. Bridges, and W. R. Ott, "Radiometric Calibrations of Portable Sources in the Vacuum Ultraviolet," *J. Res. Natl. Bur. Stand. (1934).*, vol. 93, no. 1, pp. 21–39, 1988.
[20] C. O. Laux, "Optical diagnostics and radiative emission of air plasmas," Stanford University, 1993.
[21] B. J. McBride, *Computer Program for Calculation of Complex Chemical Equilibrium Compositions and Applications*. NASA, 1996.
[22] C. O. Laux, "Radiation and nonequilibrium collisional-radiative models," *von Karman Inst. Spec. Course Physico-chemical Model. High Enthalpy Plasma Flows, Rhode-Saint-Genèse, Belgium 4–7 June 2002*, 2002.
[23] A. Tibère-Inglesse, S. McGuire, and C. O. Laux, "Nonequilibrium radiation from a recombining nitrogen plasma," *AIAA Aerosp. Sci. Meet. 2018*, no. 210059, 2018.